Method for retrieving effective properties of locally resonant acoustic metamaterials

Vladimir Fokin, Muralidhar Ambati, Cheng Sun, and Xiang Zhang*
Nano-scale Science and Engineering Center, University of California, 5130 Etcheverry Hall, Berkeley, California 94720, USA
(Received 27 April 2007; published 4 October 2007)

Acoustic metamaterials can be described by effective material properties such as mass density and modulus. We have developed a method to extract these effective properties from reflection and transmission coefficients, which can be measured experimentally. The dependency of effective properties on the positions of the boundaries of the acoustic metamaterial is discussed, and a proper procedure to determine the boundaries is presented. This retrieval method is used to analyze various acoustic metamaterials, and metamaterials with negative effective properties are reported.

DOI: 10.1103/PhysRevB.76.144302 PACS number(s): 43.20.+g, 43.90.+v, 81.05.Zx

I. INTRODUCTION

In recent decades, there has been growing interest in classical wave propagation in periodic composite materials.[1–23] Initial efforts were focused on developing the acoustic analog of photonic crystals, which are composite electromagnetic materials with highly contrasting permittivity and/or permeability layers with periodicity about the free space wavelength. Bragg-scattering based band gaps in photonic crystals[1–4] were shown to exist for elastic waves in phononic crystals, in which density and bulk modulus are modulated spatially.[5–23] Specially designed phononic crystals have been utilized in new devices such as flat acoustic lenses and acoustic multiplexers.[24–27]

Unlike phononic crystals, locally resonant acoustic metamaterials—with resonators built into individual unit cells—can exhibit anomalous behavior while utilizing lattice constants much shorter than the acoustic wavelength, thus making the effective medium approach appropriate.[28] The development of these acoustic metamaterials has led to groundbreaking demonstrations of negative acoustic properties,[29] which helped to broaden the range of material responses found in nature. These negative effective acoustic properties are dynamic and dispersive in nature. Negative bulk modulus implies that volume change is out of phase with applied dynamic pressure. Negative mass density implies that acceleration is out of phase with the dynamic pressure gradient. These negative effective properties manifest when the appropriate resonances in the metamaterial are strong enough so that the scattered field prevails over the background incident field. It was shown that a monopolar resonance creates a negative elastic modulus and a dipolar resonance creates a negative effective density at frequencies around respective resonant frequencies.[30]

Several numerical methods are available for the study of periodic composites, including the plane wave expansion method,[5–7] multiple scattering theory method,[10–13] variational method,[8] and finite difference time domain method.[9] These methods solve for the local field in the simulation domain. However, since the acoustic wavelength is much longer than the lattice constant of locally resonant acoustic metamaterials, we can instead consider the scattering in an average sense and assign macroscopic effective properties to the metamaterial. Effective properties can provide an accurate and simple description of wave interaction with the associated metamaterial.

In this paper, we present a method to extract effective properties of metamaterials from reflection and transmission coefficients that can be obtained from measurements, and discuss details of this method including the boundary position location of metamaterials and sign selection of the refractive index n and impedance z. We show the effects of the selection of boundary position on the extraction of acoustic metamaterial properties, and that one can avoid the ambiguity often associated with independent selection of signs in expressions for effective refractive index and impedance. These signs in the expressions for effective refractive index and impedance are dependent. Finally, using the retrieval method to analyze various acoustic metamaterials, we present designs of acoustic metamaterials with negative material properties.

II. RETRIEVAL METHOD FOR THE CALCULATION OF EFFECTIVE PROPERTIES

We extend a method for retrieving effective material properties of electromagnetic materials[31,32] to acoustic metamaterials. In this retrieval method, the effective refractive index n and impedance z are obtained from reflection and transmission coefficients for a plane wave normally incident on the slab. The effective mass density and sound speed are then calculated from n and z. This technique allows the use of experimental measurements to obtain metamaterial effective properties. A schematic illustrating the retrieval method is shown in Fig. 1. The metamaterial [Fig. 1(a)] is replaced by a homogeneous fluid slab of material [Fig. 1(b)] which provides the same amplitude and phase of reflection and transmission coefficients. Effective properties are obtained by using an inverse technique [Fig. 1(c)], which is discussed in this section.

Let us consider the reflection R and transmission T coefficients for a plane wave incident on a liquid acoustic layer with density ρ_2 and sound speed c_2 placed between two different media with densities ρ_1, ρ_3 and sound speeds c_1, c_3 (Ref. 33):

$$R = \frac{(Z_1 + Z_2)(Z_2 - Z_3)e^{-2i\phi} + (Z_1 - Z_2)(Z_2 + Z_3)}{(Z_1 + Z_2)(Z_2 - Z_3)e^{-2i\phi} + (Z_1 - Z_2)(Z_2 - Z_3)}, \qquad (1)$$

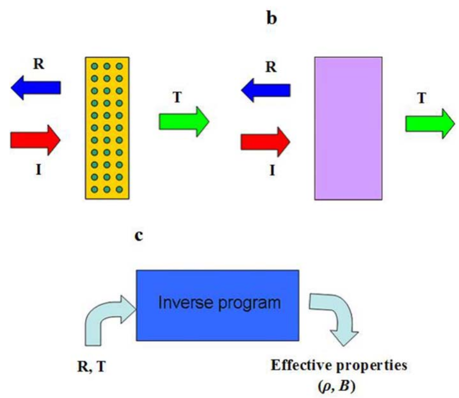

FIG. 1. (Color online) Technique used for obtaining the effective properties of a metamaterial. (a) This illustrates the system under consideration with incident, reflected, and transmitted plane waves. (b) This shows a slab of effective material equivalent to the system shown in (a) at a selected frequency. (c) This illustrates a technique used for obtaining effective properties of a metamaterial.

$$T = \frac{4Z_1Z_2}{(Z_1 - Z_2)(Z_2 - Z_3)e^{i\phi} + (Z_1 + Z_2)(Z_2 + Z_3)}. \tag{2}$$

In these equations, $Z_i = \rho_i c_i / \cos \vartheta_i$ is the acoustic impedance, ϑ_i the angle between the wave vector and layer normal, $\phi = \pi f d \cos \vartheta_2 / c_2$ the phase change across the layer, f the frequency of acoustic wave, and d the slab thickness. For the simplified case of plane waves normally incident on a slab with identical media on both sides, the reflection and transmission coefficients reduce to

$$R = \frac{Z_2^2 - Z_1^2}{Z_1^2 + Z_2^2 + 2iZ_1Z_2 \cot \phi}, \tag{3}$$

$$T = \frac{1 + R}{\cos \phi - \dfrac{Z_2 i \sin \phi}{Z_1}}. \tag{4}$$

Introducing $m = \rho_2 / \rho_1$, $n = c_1 / c_2$, $k = \omega / c_1$, and $\xi = \rho_2 c_2 / \rho_1 c_1$, we obtain

$$R = \frac{\tan(nkd)\left(\dfrac{1}{\xi} - \xi\right)i}{2 - \tan(nkd)\left(\dfrac{1}{\xi} + \xi\right)i}, \tag{5}$$

$$T = \frac{2}{\cos(nkd)\left[2 - \tan(nkd)\left(\dfrac{1}{\xi} + \xi\right)i\right]}. \tag{6}$$

These formulas are identical to formulas obtained for the electromagnetic field.[31,32] By inverting Eqs. (5) and (6), we obtain acoustic impedance ξ and refractive index n,

$$n = \frac{\pm \cos^{-1}\left(\dfrac{1}{2T}[1 - (R^2 - T^2)]\right)}{kd} + \frac{2\pi m}{kd}, \tag{7}$$

$$\xi = \pm \sqrt{\frac{(1 + R)^2 - T^2}{(1 - R)^2 - T^2}}, \tag{8}$$

where m is the branch number of $\cos^{-1}$ function. As can be seen from Eqs. (7) and (8), both impedance and refractive index are complex functions of complex variables. Mathematically, any combination of signs in Eqs. (7) and (8) and any m result in the same values for reflection and transmission coefficients. These issues can be resolved by imposing additional constraints on the metamaterial properties. Passive metamaterials require that the real part of ξ be positive, which determines the sign in Eq. (8). In addition, a positive imaginary sound speed component is required, restricting the imaginary part of n to negative values.

Though these conditions seem independent, careful examination of Eqs. (7) and (8) shows that the signs in these equations are dependent. When $\mathrm{Re}(\xi)$ or $\mathrm{Im}(n)$ is close to zero, errors in measurement or calculation of reflection and transmission coefficients may cause incorrect combinations of signs in Eqs. (7) and (8). This would create discontinuities in n and z with frequency. To overcome this problem, we rewrite Eqs. (7) and (8) in the form

$$\xi = \frac{r}{1 - 2R + R^2 - T^2}, \quad n = \frac{-i \log x + 2\pi m}{kd}, \tag{9}$$

where

$$r = \mp \sqrt{(R^2 - T^2 - 1)^2 - 4T^2}, \quad x = \frac{(1 - R^2 + T^2 + r)}{2T}. \tag{10}$$

We begin by solving the right-hand side of the expression for r, and we select whichever of the two roots yields a positive solution for $\mathrm{Re}(\xi)$. This value of r used in the expression for x eliminates its ambiguity in the expression for n. This procedure provides consistent results and allows one to avoid nonphysical solutions due to incorrect selection of second sign in Eqs. (7) and (8). However, the determination of $\mathrm{Re}(n)$ from Eq. (5) is complicated by the fact of choosing the proper value of m. Moreover, for thick metamaterials, the solutions of n for different values of m can lie close to each other. This problem of selecting the branch number m can be circumvented by determining the effective parameters of a minimum thickness metamaterial, for which m is zero. Using this solution, the sign and branch number for increasing frequency can be determined from the requirement of continuous n provided the frequency steps are small enough to account for metamaterials being highly dispersive.

III. DETERMINATION OF METAMATERIAL THICKNESS

Another important issue in obtaining the effective material properties is the determination of positions of metamaterial boundaries. The phase of reflected and transmitted waves

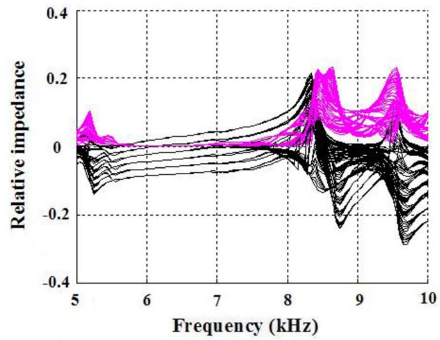

FIG. 2. (Color online) Frequency dependence of effective impedance of a metamaterial on the boundary position of an acoustic metamaterial. Effective impedance is sensitive to the boundary positions of a metamaterial. Magenta and black colors correspond to real and imaginary parts of impedance, respectively, and different lines correspond to different positions of left and right boundaries for the metamaterial from the edge of the outer cylinder to twice the length of the unit cell. The metamaterial under consideration consists of hollow soft silicon rubber cylinders arranged in a square lattice with 1 cm lattice constant and 2 mm inner radius. The ratio of inner and outer radii of the cylinder is equal to 2. The sound speed in the resin is taken as 33 m/s, with the imaginary part of the sound speed equal to 1% of the real part.

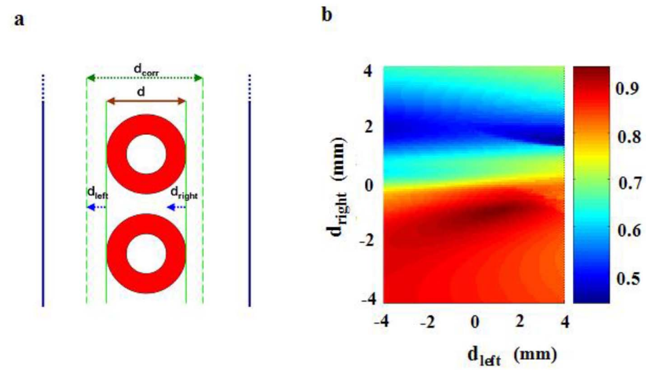

FIG. 3. (Color online) A proper procedure to determine the boundary positions of the metamaterial. (a) Geometry of the metamaterial under consideration, showing the initial metamaterial thickness d and corrected thickness (d_{corr}=d_{left}-d_{right}+d). The arrow directions show the positive displacements of the boundaries. (b) Plot of a weight function Ψ given in Eq. (11) shows a maximum corresponding to the boundaries at the unit cell. Vertical and horizontal axes correspond to the positions of the right and left boundaries of the metamaterial. The abscissa in (b) corresponds to displacement of front boundary, and the beginning of the coordinates was set on the edge of the cylinder. Calculations were made for metamaterials with one and two columns of unit cells using acoustic impedance as the material property.

should be measured at the surfaces of the metamaterial, which are not well defined. The importance of boundary positions is illustrated using a metamaterial constructed from hollow silicone rubber cylinders immersed in water. The extracted effective impedance of this metamaterial is shown in Fig. 2, with different lines corresponding to different positions of left and right boundaries for the metamaterial. The variation of impedance with effective thickness of the metamaterial—ranging from outer radius of cylinder to double size of unit cell—confirms that improper boundary positions can lead to variations of an order in magnitude in effective properties.

The ambiguity in boundary positions is resolved by using the constraint that slabs of the metamaterial with different thicknesses should have the same effective properties. Effective properties for two metamaterial slab thicknesses are determined over a wide frequency range as a function of boundary distance from the cylinder surface. The weight function Ψ provides a frequency averaged measure of the difference in effective properties between the two slabs as a function of boundary position,

$$\Psi(d_{left},d_{right}) = 1 - \frac{1}{nf}\sum_{1}^{nf}\left[\frac{\mathrm{abs}(P_1(f,d_{left},d_{right}) - P_2(f,d_{left},d_{right}))}{\max(P_1,P_2)}\right]. \tag{11}$$

In Eq. (11), indices 1,2 correspond to two slabs of the metamaterial of different thicknesses, $P_{1,2}$ is the effective property of the metamaterial, d_{left}, d_{right} are the displacements of effective boundaries of the metamaterial from the cylinder surface, and nf is the total number of frequencies. The weight function is maximized when the difference in effective properties is minimum; therefore, the coordinates of maxima on the d_{left}, d_{right} plane give the left and right boundary positions of the metamaterial.

The procedure is demonstrated using the metamaterial constructed from hollow soft silicon cylinders with relevant geometric parameters shown in Fig. 3(a). One weight function calculated using effective impedance as the property is shown in Fig. 3(b). Though the weight function has an ellipselike form around the maximum, meaning different sensitivities to the "front" and "back" boundary positions, it was found that the metamaterial boundary positions are approximately the unit cell boundary. Repetition for several different slab thicknesses confirmed the same finding. To demonstrate the effectiveness of this procedure, the frequency dependence of impedance for two different thicknesses of metamaterial before and after the determination of the metamaterial boundary position is shown in Figs. 4(a) and 4(b). The initial boundary positions coincide with the surface of the cylinders, while the final positions are close to the boundary of the unit cell. Both real and the imaginary parts of the impedance coincide very well after the determination of the boundary positions.

The presented method was adapted as a computer code and tested rigorously for retrieval properties of a slab with known properties. The reconstructed values of c and ρ show excellent agreement with exact values. Average absolute error was equal to 10^{-8} when analytically calculated reflection and transmitted coefficients were used, and 10^{-6} when reflection and transmission coefficients were obtained from finite element modeling data.[34]

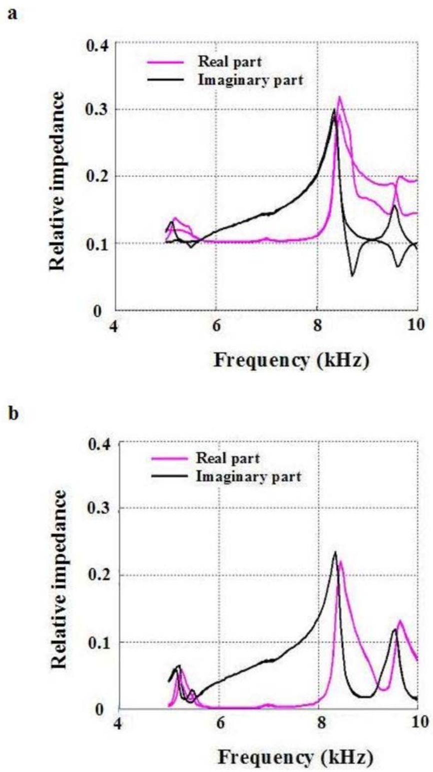

FIG. 4. (Color online) Effective impedance for two slabs of acoustic metamaterial constructed from hollow soft silicon rubber cylinders with different thicknesses (a) before optimization of boundary position and (b) after optimization of boundary position. Effective impedance is independent of the thickness of the metamaterial, formed by one and two columns of hollow cylinders, after optimizing the boundary positions. Magenta line corresponds to the real part of the impedance, and black line corresponds to the imaginary part of the impedance.

IV. ANALYSIS OF ACOUSTIC METAMATERIALS USING THE RETRIEVAL METHOD

We have used the rigorous method developed to analyze different acoustic metamaterials for possible negative effective material properties. In this section, we report two acoustic metamaterials showing negative effective acoustic properties over certain frequency ranges. In these calculations, we set the imaginary part of sound speed in the soft material equal to 1% of the real part.

The first design is the soft silicon rubber hollow cylinders immersed in water mentioned earlier. The 2 to 1 outer/inner radii ratio cylinders are placed in a square lattice with an inner radius of 2 mm and a lattice constant equal to 1 cm. In the calculated frequency dependency of the effective refractive index shown in Fig. 5, a narrow frequency band of negative index is seen around 7000 Hz. However, concurrent with this negative real refractive index component of around -1 is an imaginary component several times larger. This indicates that the negative index is loss based, in contrast to the situation where negative index is obtained with simultaneous negative mass density and negative bulk modulus. In this design, the real part of the effective mass density is positive

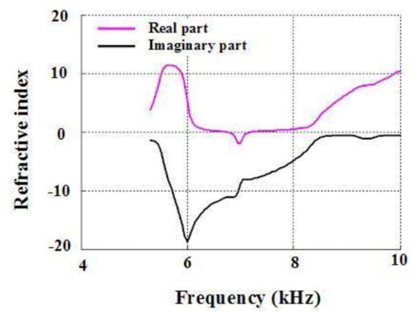

FIG. 5. (Color online) Effective refractive index of acoustic metamaterial consisting of hollow soft silicon rubber cylinders in water. The configuration is the same as presented in earlier figures. A narrow frequency band of negative index is seen around 7000 Hz. The negative index obtained is loss based, which is different from the double negative acoustic medium.

whereas that of bulk modulus is negative. In addition, the large imaginary components of the material properties are sufficient to cause a net negative effective index. This situation is analogous to that of electromagnetic metamaterials.[35]

The second metamaterial design is composed of rectangular rods of soft silicon rubber attached to rigid rods arranged in a square lattice with a 4 mm lattice constant. Intuitively, this design could have negative mass density, since the asymmetric boundary condition will cause the soft silicon rubber center of mass to move out of phase with the external pressure field at resonance. Retrieval of effective properties using our method confirms the existence of a narrow frequency region, in which the mass density is negative (Fig. 6). The negative mass density peaks near $-1000\ \mathrm{kg/m^3}$, equaling the magnitude of density of the surrounding liquid. It should be noted in Fig. 6 that the imaginary part of density changes sign with frequency. This should not be interpreted as changing from attenuation to gain, as that is dependent on the imaginary part of the sound speed. The sign change in the imaginary part of the effective density simply coincides with a change in the phase of reflected and transmitted acoustic

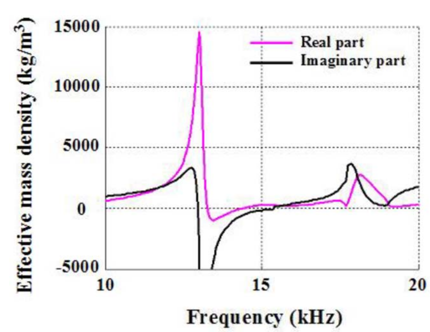

FIG. 6. (Color online) Effective mass density of an acoustic metamaterial consisting of rectangular rods of soft resin (2 mm height and 1.5 mm width) attached to rigid rods of the same dimensions in water. The unit cells are arranged in a square lattice with a lattice constant of 4 mm. A narrow frequency band around 13 kHz shows a negative effective mass density equal in magnitude to the density of water.

waves. Finite element simulations[32] confirm this fact.

Metamaterials with negative properties lead to interesting phenomena such as negative refraction[30] and new surface resonances,[36] which will be useful in sub-diffraction-limited imaging in acoustics. For example, a metamaterial with negative density equal in magnitude to the density of the surrounding liquid for longitudinal acoustic waves will behave in a similar way as the materials with negative permittivity in an electromagnetic field. Such an acoustic metamaterial can be used as a "superlens" in acoustics.

V. CONCLUSION

A retrieval method of obtaining effective properties of acoustic metamaterials from reflection and transmittance coefficients is presented. It is shown that sign and branch number selection can be obtained using passive metamaterial assumptions coupled with the condition of a continuous index. The influence of metamaterial boundary positions is investigated, and a proper procedure is presented to obtain the correct boundary position. Two metamaterials designs—one with negative density and the other with negative index—are analyzed using this retrieval method.

ACKNOWLEDGMENTS

Financial support from the ONR (Grant No. N000140710626) is acknowledged. The authors also acknowledge helpful discussions with Lee Fok.

*Corresponding author; xiang@berkeley.edu

[1] E. Yablonovitch, Phys. Rev. Lett. **58**, 2059 (1987).
[2] K. M. Ho, C. T. Chan, and C. M. Soukoulis, Phys. Rev. Lett. **65**, 3152 (1990).
[3] X. D. Wang, X. G. Zhang, Q. Yu, and B. Harmon, Phys. Rev. B **47**, 4161 (1993).
[4] W. M. Robertson, G. Arjavalingam, R. D. Meade, K. D. Brommer, A. M. Rappe, and J. D. Joannopoulos, Phys. Rev. Lett. **68**, 2023 (1992).
[5] M. Sigalas and E. N. Economou, Solid State Commun. **86**, 141 (1993).
[6] M. S. Kushwaha, P. Halevi, L. Dobrzynski, and B. Djafari-Rouhani, Phys. Rev. Lett. **71**, 2022 (1993).
[7] F. R. Montero de Espinosa, E. Jimenez, and M. Torres, Phys. Rev. Lett. **80**, 1208 (1998).
[8] C. Goffaux and J. Sanchez-Dehesa, Phys. Rev. B **67**, 144301 (2003).
[9] Y. Tanaka, Y. Tomoyasu, and S. I. Tamura, Phys. Rev. B **62**, 7387 (2000).
[10] I. E. Psarobas, N. Stefanou, and A. Modinos, Phys. Rev. B **62**, 278 (2000).
[11] Z. Liu, C. T. Chan, P. Sheng, A. L. Goertzen, and J. H. Page, Phys. Rev. B **62**, 2446 (2000).
[12] J. Mei, Z. Liu, J. Shi, and D. Tian, Phys. Rev. B **67**, 245107 (2003).
[13] Y. Y. Chen and Z. Ye, Phys. Rev. E **64**, 036616 (2001).
[14] M. M. Sigalas and E. N. Economou, J. Sound Vib. **158**, 377 (1992).
[15] M. M. Sigalas and N. Economou, Europhys. Lett. **36**, 241 (1996).
[16] M. M. Sigalas and N. Garcia, Appl. Phys. Lett. **76**, 2307 (2000).
[17] J. O. Vasseur, P. A. Deymier, B. Chenni, B. Djafari-Rouhani, L. Dobrzynski, and D. Prevost, Phys. Rev. Lett. **86**, 3012 (2001).
[18] P. Lambin, A. Khelif, J. O. Vasseur, L. Dobrzynski, and B. Djafari-Rouhani, Phys. Rev. E **63**, 066605 (2001).
[19] S. X. Yang, J. H. Page, Z. Liu, M. L. Cowan, C. T. Chan, and P. Sheng, Phys. Rev. Lett. **88**, 104301 (2002).
[20] M. S. Kushwaha, P. Halevi, G. Martínez, L. Dobrzynski, and B. Djafari-Rouhani, Phys. Rev. B **49**, 2313 (1994).
[21] M. Kafesaki, M. Sigalas, and E. N. Economou, Solid State Commun. **96**, 285 (1995).
[22] M. Kafesaki and E. N. Economou, Phys. Rev. B **52**, 13317 (1995).
[23] R. Martinez-Sala, J. Sancho, J. V. Sanchez, V. Gomez, J. Llinares, and F. Meseguer, Nature (London) **378**, 241 (1995).
[24] F. Cervera, L. Sanchis, J. V. Sánchez-Pérez, R. Martínez-Sala, C. Rubio, F. Meseguer, C. López, D. Caballero, and J. Sánchez-Dehesa, Phys. Rev. Lett. **88**, 023902 (2001).
[25] Y. Pennec, B. Djafari-Rouhani, J. O. Vasseur, A. Khelif, and P. A. Deymier, Phys. Rev. E **69**, 046608 (2004).
[26] D. Torrent, A. Hakansson, F. Cervera, and J. Sanchez-Dehesa, Phys. Rev. Lett. **96**, 204302 (2006).
[27] A. Hakansson, J. Sanchez-Dehesa, and L. Sanchis, Phys. Rev. B **70**, 214302 (2004).
[28] Z. Liu, X. Zhang, Y. Mao, Y. Y. Zhu, Z. Yang, C. T. Chan, and P. Sheng, Science **289**, 1734 (2000).
[29] N. Fang, D. Xi, J. Xu, M. Ambati, W. Srituravanich, C. Sun, and X. Zhang, Nat. Mater. **5**, 452 (2006).
[30] J. Li and C. T. Chan, Phys. Rev. E **70**, 055602(R) (2004).
[31] D. R. Smith, S. Schultz, P. Markos, and C. M. Soukoulis, Phys. Rev. B **65**, 195104 (2002).
[32] X. Chen, T. M. Grzegorczyk, B. I. Wu, J. Pacheco, and J. A. Kong, Phys. Rev. E **70**, 016608 (2004).
[33] L. Brekhovskikh, *Waves in Layered Media* (Academic, New York, 1980).
[34] FEMLAB Modeling Guide, Version 3.1i, Comsol AB, Stockholm, Sweden, 2004.
[35] T. G. Mackay and A. Lakhtakia, Microwave Opt. Technol. Lett. **47**, 313 (2005).
[36] M. Ambati, N. Fang, C. Sun, and X. Zhang, Phys. Rev. B **75**, 195447 (2007).